Materials Chemistry Horizons RESEARCH

Fabrication and Optical Properties Study of Poly(*m*-Phenylene diamine)/ Sulfonated Single-Walled Carbon Nanotubes Nanocomposite

Saman Rahimi[1], and Yasser Rajabi[2*]

[1]School of Chemistry, Damghan University, Damghan, Iran
[2]School of Physics, Damghan University, Damghan, Iran

***Corresponding author**: y.rajabi@du.ac.ir (Y. Rajabi)

Mater. Chem. Horizons, 2023, 2(4), 283-292 10.22128/MCH.2023.763.1051 OPEN ACCESS

ABSTRACT

A poly(m-phenylene diamine) (PmPDA)/sulfonated single-walled carbon nanotubes (SWCNT-SO_3H) nanocomposite was synthesized via in situ polymerization. Successful incorporation of SWCNT-SO_3H into the PmPDA matrix was confirmed through Fourier transform infrared spectroscopy, X-ray diffraction, energy-dispersive X-ray spectroscopy, scanning electron microscopy, UV-visible spectroscopy, and thermogravimetric analysis. The nanocomposite exhibited a red shift of 6 nm in the UV-visible spectrum compared to the pristine polymer, attributed to the conductivity of the incorporated nanotubes. The thermogravimetric analysis also showed improved thermal stability for the nanocomposite over the polymer. Importantly, the nonlinear optical properties were studied via Z-scan measurements. The nanocomposite displayed a nonlinear refractive index on the order of 10^{-3} m^2/W and a nonlinear absorption coefficient on the order of 10^{-5} m/W, demonstrating self-defocusing behavior. Varying the concentration from 0.3 to 0.7 mg/mL and input laser intensity from 6.2 to 164.5 mW/cm^2 tuned the optical nonlinearity. Overall, the easy integration of carbon nanotubes makes the PmPDA nanocomposite a useful self-defocusing material for optical limiting and switching applications.

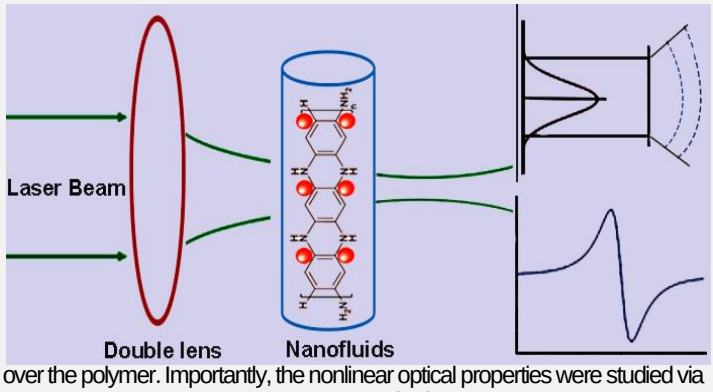

Keywords: Optical properties, poly(m-phenylene diamine), sulfonated singel-walled carbon nanotubes, nanocomposite

1. Introduction

In the realm of materials science and polymer nanocomposites, the amalgamation of distinct components to develop novel materials has led to groundbreaking advancements [1]. Poly(m-phenylene diamine) (PmPDA), a member of the aromatic amine polymer family, stands as an intriguing material known for its exceptional properties. Its structure, characterized by the presence of phenyl rings linked by diamine moieties, contributes to its intrinsic conductivity, mechanical robustness, and thermal stability[2]. These attributes render PmPDA a promising candidate in various technological applications, spanning from electronics to biomedical engineering[3].On the other hand, the advent of nanotechnology has fostered the exploration of carbon-based nanomaterials. Singel-walled carbon nanotubes (SWCNTs) have received considerable interest for their extraordinary mechanical, electrical, and optical properties [4]. However, pristine carbon nanotubes are hydrophobic and tend to aggregate due to strong van der Waals interactions, limiting their utilization in composites. Surface functionalization of carbon nanotubes has been shown to improve dispersion and interfacial interactions with polymer matrices. Sulfonated single-walled carbon nanotubes (SWCNT-SO_3H) feature anionic groups that can interact with cationic polymers through electrostatic interactions [5]. In recent years, many studies on the optical properties of nanocomposites have been made based on conductive polymers. Dhole and Co-workers studied the optical properties of a nanocomposite of polyaniline with ZnO nanoparticles [6]. Khairy et al. studied the optical and electrical properties of a polyaniline nanocomposite with nickel ferrite nanoparticles [7]. Zhang et al. investigated dielectric properties and piezoelectric properties of a nanocomposite of poly(vinylidene difluoride) and graphite for use in lasers [8]. Nowruzi and coworkers investigated the nonlinear

Received: December 17, 2023
Received in revised: December 29, 2023
Accepted: December 31, 2023

properties of nanofluids made from poly(aniline-co-pyrrole) zinc oxide [9]. Dadkhah et al studied the enhancement of thermo-optical properties of poly (aniline-co-ortho phenylenediamine)@TiO_2[10]. Liu and co-workers investigated a one-dimensional coordination polymer [11]. Muller et al. focus on the optical limiting behavior of a series of polymer-dye nonlinear nanocomposites [12].

Therefore, the merging of PmPDA with SWCNT-SO_3H engenders a new paradigm in the realm of nanocomposites. The synergistic interplay between these constituents holds immense promise, offering a platform to explore and harness a spectrum of advantageous properties, particularly in the realm of optics. The blending of these materials aims not only to enhance the intrinsic properties of the individual components but also to explore and engineer new functionalities that arise from their unique synergy.

This study endeavors to fabricate a poly(m-phenylene diamine)/sulfonated Multi-walled Carbon Nanotubes (PmPDA/SWCNT-SO_3H) nanocomposite and systematically investigate its optical properties. By meticulously characterizing and analyzing the optical behavior, this research aims to elucidate the impact of SWCNT-SO_3H on the optical properties of PmPDA and delineate the potential applications of this nanocomposite in various optoelectronic and photonic domains.

2. Materials and methods

2.1. Materials and instruments

Meta-phenylenediamine with 98% purity, ammonium persulfate with 98% purity, hydrochloric acid, 37% dimethyl sulfoxide, 98% sulfuric acid, and tetrahydrofuran were purchased from Merck, Germany. Single-wall carbon nanotubes (SWCNTs) were purchased from Neutrino (Iran).

A Fourier transform infrared spectrometer (FTIR) model PerkinElmer, made in Germany, was used to study the chemical structure of the samples in the range of 4000-400 cm^{-1}. Crystallinity behavior and irregularities of samples were studied by X-ray diffraction (XRD model Bruker D8 Advance) made in Germany with a scanning speed of 5°/min in the range of 5-80°. Field emission scanning electron microscopy with an energy dispersive X-ray spectroscopy detector, MIRA3 XMU model (FE-SEM/EDX) made in the Czech Republic, was used to study morphology and elemental composition. The thermal stability of samples was studied with a thermogravimetric analyzer (TGA) model TG209F3 from NETZSCH, made in Germany, with a heating rate of 10°C/min under argon. The optical properties of samples were studied with a Cecil 5000 ultraviolet-visible (UV-vis) spectrometer made in England. Linear and nonlinear optical properties were studied using a Z-scan device and solid-state neodymium-doped yttrium aluminum garnet (Nd: YAG) laser made in Iran with an output of green light at a wavelength of 532nm.

2.2. Sulfonation of carbon nanotubes (SWCNT-SO_3H)

Sulfonation of carbon nanotubes was performed based on the reports presented in relevant articles (**Figure 1a**) [13]. 0.4 g of SWCNT was added to a flask containing 14 mL of a 1:1 volume ratio sulfuric acid and nitric acid mixture and placed on a magnetic stirrer for 5 hours. Then, the reaction container was placed in an ultrasonic bath for 15 minutes. The contents of the flask were then washed with distilled water to neutral pH using a centrifuge and placed in an oven at 70 °C for 12 hours to dry. After that, the dried material was mixed with 2 mL of sulfuric acid and placed under a hot water bath at 70 °C on a magnetic stirrer for 2 hours. In the end, the obtained sediment was washed several times with distilled water using a centrifuge and dried in an oven at 70 °C.

2.3. Fabrication of poly(meta-phenylenediamine)/SWCNT-SO_3H (PmPDA/SWCNT-SO_3H)

In Poly(meta-phenylenediamine)/SWCNT-SO_3H nanocomposites with different weight percentages of SWCNT-SO_3H (5% and 10%) were fabricated by an in situ polymerization method (**Figure 1b**). First, 1 g of meta-phenylenediamine monomer was dissolved in 50 mL of hydrochloric acid (1 M). Then, 0.1 g of SWCNT-SO_3H nanoparticles were poured into 5 mL of distilled water and placed in an ultrasonic bath for 15 minutes to disperse the nanoparticles. In the next step, the mixture containing the nanoparticles was gradually added to the vessel containing the monomer. In another separate container, 2.11 g of APS initiator was dissolved in 20 mL of distilled water and added dropwise to the container containing monomer and nanoparticles over 15 minutes. The resulting solution was placed on a magnetic stirrer at room temperature for 24 hours to form the final composite. Next, the obtained sediment

was washed with water and acetone and separated by centrifuge, and finally, the obtained sediment was dried at room temperature.

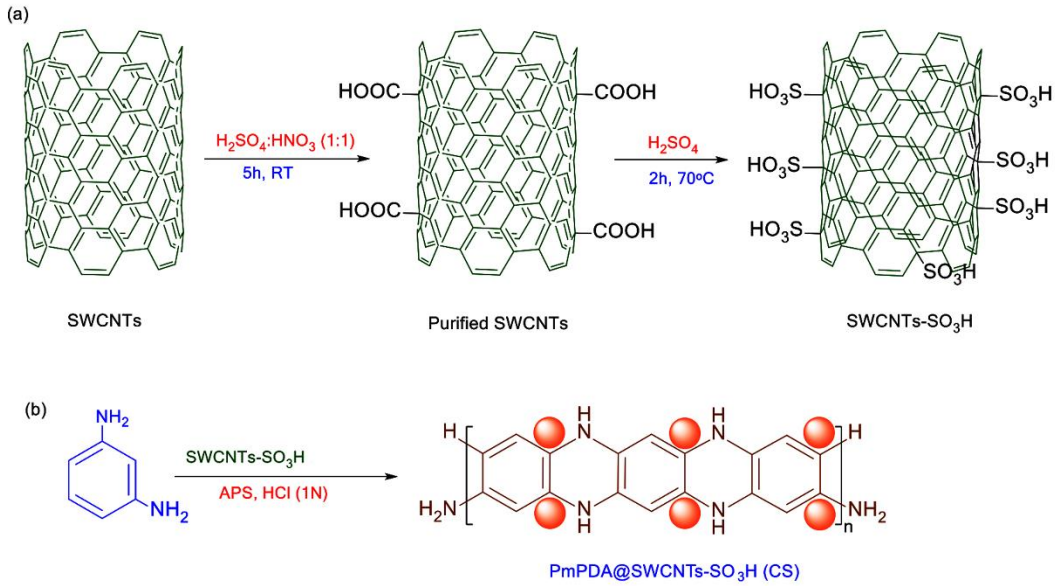

Figure 1. Schematic of sulfonation of carbon nanotubes (**a**) and preparation of nanocomposite (**b**).

2.4. Collecting data from samples using the Z-scanning method

The nonlinear properties of materials were evaluated by the Z-scan method. In this research, a Gaussian beam from a continuous Nd: YAG laser with a wavelength of 532 nm, with a power of 165 mW, and a beam waist diameter of 5.6×10^{-6} m was focused to a doublet lens with a focal distance of 19 cm on a 1 mm thick cell containing the nonlinear material. During the path before reaching the focal point, intensity filters were used to attenuate the optical power of the laser to 6.2, 17, 57.44, and 164.5 mW to evaluate the nonlinear refractive index and nonlinear absorption coefficient of the materials. In this method, three intensity detectors, D_2 is the closed aperture, D_3 is the open aperture, and D_1 measures the light intensity before the focal point. When executing the Z-scan setup, data collection was performed with a MATLAB program, recording and storing the intensity changes with an intensity detector (PM100).

2.5. Nonlinear absorption coefficient

An open-aperture light receiver was used to measure the nonlinear absorption coefficient of the samples by the Z-scan method. In this way, instead of an aperture, a lens captures all light transmitted through the thin sample. In this method, as the light beam passes through the focal point of the sample area, the detector measures the total transmitted intensity. The normalized change in transmitted intensity is obtained using equation (1) [10]:

$$\beta = \frac{2^{3/2}[\Delta T]}{I_0 L_{eff}} \qquad (1)$$

In this equation, ΔT is the difference between the peak and valley in the graphs, I_0 is the intensity of the laser light at the focal point, and L_{eff} is the effective length of the sample, which is obtained from the following equation[10], where α is the linear absorption coefficient obtained from the UV-Vis spectrum.

$$L_{eff} = \left(\frac{1-e^{-\alpha L}}{\alpha}\right) \qquad (2)$$

2.6. Nonlinear refractive index

A closed aperture light receiver was used to measure the nonlinear refractive index of the samples by the Z-scan method. In this method, as the sample passes through the focal beam area, the detector measures the fraction of

intensity passing through both the aperture and the sample. In this case, the detector shows measured maximum and minimum light intensity. The magnitude of the phase change can be obtained from the normalized transmittance change ΔT_{pv} using equation (3) [14]:

$$|\Delta\Phi_0| = \frac{\Delta T_{p-v}}{0.406(1-s)^{0.27}} \quad (3)$$

In this equation, s is the fraction of the beam transmitted through the aperture. When the light received by the detector shows a minimum and maximum value, or the so-called peak and valley, the following equation can be used to obtain the nonlinear refractive index [14].

$$n_2 = \frac{\Delta T}{0.406 K I_0 L_{eff}} \quad (4)$$

3. Results and discussion

3.1. Characterization

FT-IR spectroscopy: The molecular structure of the samples was investigated by FT-IR spectroscopy. As shown in **Figure 2**, in the spectrum related to PmPDA, two peaks between 3111-3411 cm^{-1} are related to the stretching vibration of N-H bonds. The absorption peaks at 1651 cm^{-1} and 1511 cm^{-1} can be attributed to the stretching vibrations of quinoid and benzenoid structures, respectively[15]. The corresponding peak in the region of 1551 cm^{-1} is related to C-N bond vibrations [15]. A comparison of the spectra of SWCNTs and SWCNTs-SO_3H shows that in the FT-IR spectrum of SWCNTs, there is a peak around 1651 cm^{-1} which can be related to carbonyl stretching vibrations [16]. This is a common feature related to the oxidation of SWCNTs, which has been reported by many other research groups [16]. The peak in the region of 3441 cm^{-1} is related to the stretching vibrations of the hydroxyl group in COOH. In the FT-IR spectrum of SWCNTs-SO_3H, one of the most obvious changes is observed in the range of 1611 cm^{-1} to 1011 cm^{-1}, which indicates modifications of carboxyl groups. Peaks in the regions of 1390 cm^{-1} and 1090 cm^{-1} are related to the asymmetric and symmetric vibrations of SO_2 in the -SO_2OH group, respectively [16]. The peaks at 684 cm^{-1} and 551 cm^{-1} are related to S=O and C-S stretching vibrations, respectively. The presence of indicator peaks related to SWCNTs-SO_3H and PmPDA in the composite spectrum indicates the successful preparation of the composite.

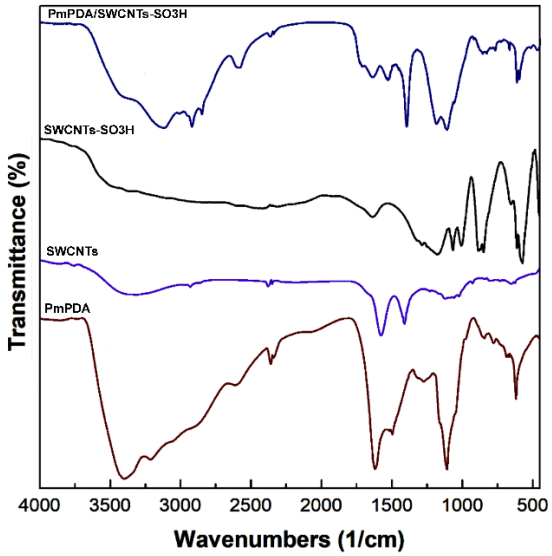

Figure 2. FTIR spectra of PmPDA, SWCNTs, SWCNTs-SO_3H, and PmPDA/SWCNTs-SO_3H nanocomposite.

X-ray diffraction (XRD): X-ray diffraction patterns were used to characterize the crystallinity of the samples. **Figure 3** shows the X-ray diffraction patterns of PmPDA, SWCNTs-SO_3H, and PmPDA/SWCNTs-SO_3H. The XRD pattern

related to PmPDA shows a semi-crystalline structure with peaks at 25, 29, 39, and 53 degrees [17]. The XRD patterns related to the SWCNTs-SO_3H sample show a fully crystalline structure [18]. The XRD pattern related to the composite sample is more similar to the PmPDA pattern with very minor changes, which indicates that the presence of SWCNTs-SO_3H nanoparticles does not significantly change the crystallinity of the composite.

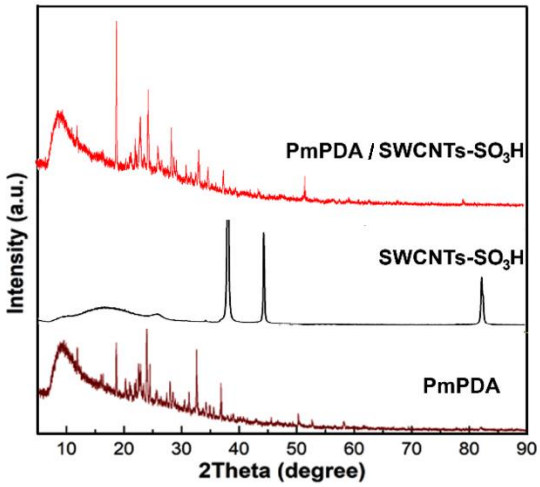

Figure 3. XRD patterns of PmPDA, SWCNTs-SO_3H, and PmPDA/SWCNTs-SO_3H nanocomposite.

Energy-dispersive X-ray (EDX) spectroscopy: In addition to FT-IR spectroscopy, energy-dispersive X-ray (EDX) spectroscopy was also utilized to confirm successful sample synthesis. **Figure 4** shows the EDX spectra for PmPDA, SWCNTs-SO_3H, and PmPDA/SWCNTs-SO_3H. The presence of N and C elements in the EDX spectrum of the PmPDA sample indicates the structure of PmPDA. The presence of S, Cl, and O elements in the polymer is due to the presence of a HCl acid solution and ammonium persulfate initiator utilized in the polymer synthesis. The presence of C, O, and S elements in SWCNTs-SO_3H indicates the successful synthesis of this material [18]. The presence of C, O, and S elements in the composite EDX spectrum proves the incorporation of SWCNTs-SO_3H nanoparticles into the composite.

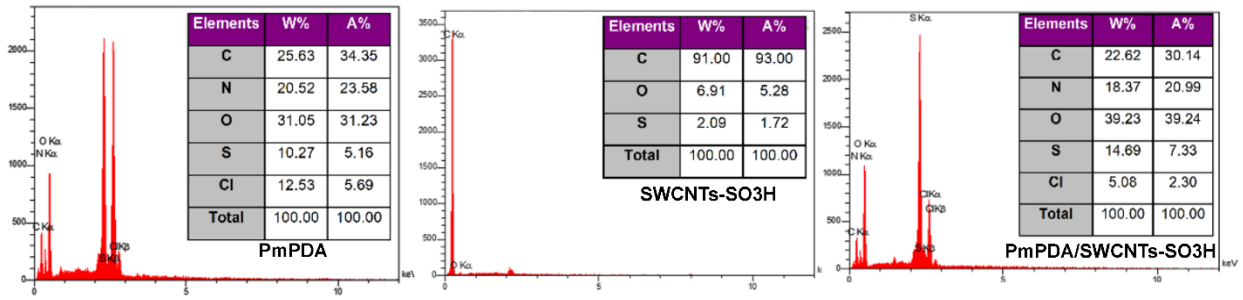

Figure 4. EDX spectra of PmPDA, SWCNTs-SO_3H, and PmPDA/SWCNTs-SO_3H nanocomposite.

Scanning electron microscope (SEM) images: A scanning electron microscope was used to examine the morphology of the samples. **Figure 5** shows 500 nm magnification SEM images of SWCNTs-SO_3H, PmPDA, and PmPDA/SWCNTs-SO_3H samples. Irregular and aggregated structures with diameters between 200 and 400 nm can be seen in the PmPDA sample SEM image [19]. Tubular structures that were deformed or broken in some areas (due to functionalization) are observed in the SWCNTs-SO_3H SEM image, indicating nanotube diameters between 10 and 20 nm [16]. The dispersion of functionalized carbon nanotubes on the polymer surface in the composite SEM image indicates the presence of carbon nanotubes in the composite.

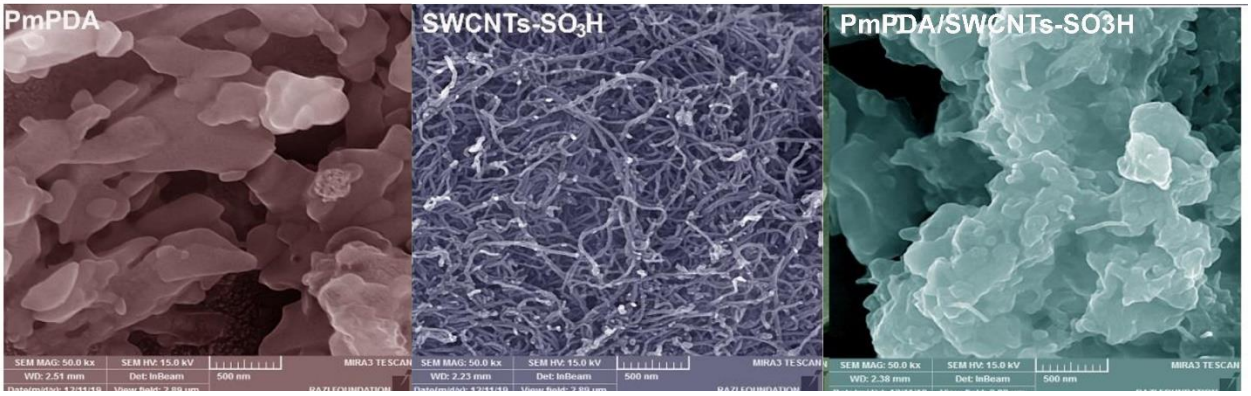

Figure 5. SEM images of PmPDA, SWCNTs-SO_3H, and PmPDA/SWCNTs-SO_3H nanocomposite.

UV-Vis spectroscopy: Ultraviolet-visible spectroscopy was utilized to study the optical properties of the prepared samples. **Figure 6** shows the UV-Vis spectra of PmPDA, SWCNTs-SO_3H, and PmPDA/SWCNTs-SO_3H samples. In the PmPDA spectrum, the peak observed at 335 nm is related to $\pi \rightarrow \pi$ transitions of quinoid rings and is associated with the degree of conjugation between phenyl rings along the polymer chain [20]. In the SWCNTs-SO_3H spectrum, there are two peaks at 251 nm (visible region) and 351 nm, corresponding to C=C bonds and the presence of sulfone groups on the nanotube surface, respectively [21]. The PmPDA/SWCNTs-SO_3H composite spectrum shows that due to the incorporation of SWCNTs-SO_3H nanoparticles, the 335 nm region peak in the PmPDA polymer is slightly red-shifted to 341 nm. These changes can be attributed to the conductivity of the sulfonated carbon nanotubes.

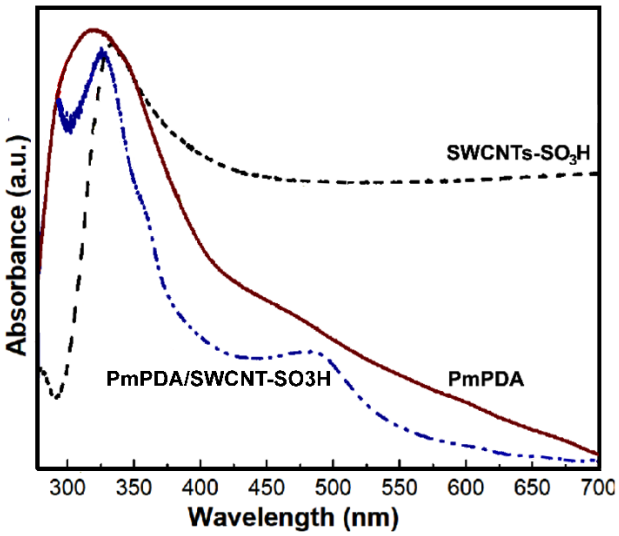

Figure 6. UV-Vis spectra of PmPDA, SWCNTs-SO_3H, and PmPDA/SWCNTs-SO_3H nanocomposite.

Thermogravimetric analysis (TGA): Thermogravimetric analysis (TGA) was utilized to study the thermal stability of the samples. **Figure 7** shows the TGA curves of PmPDA, SWCNTs-SO3H, and PmPDA/SWCNTs-SO_3H samples. In the PmPDA TGA curve, two weight losses were observed in the temperature ranges of 100-280°C and 350-700°C. The first weight loss is attributed to residual water, HCl, and oligomers. The second weight loss is related to the removal and destruction of NH_2 pendant groups and the decomposition of benzenoid and quinoid units in the PmPDA chain [22]. In the SWCNTs-SO_3H TGA curve, two weight losses occurred above 100°C and 400°C, corresponding to moisture/solvent loss and decomposition of -SO_3H groups on the carbon nanotube surface, respectively [16,23]. In the PmPDA/SWCNTs-SO_3H curve, an increase in stability is observed compared to PmPDA, which is due to the presence of SWCNTs-SO_3H nanoparticles.

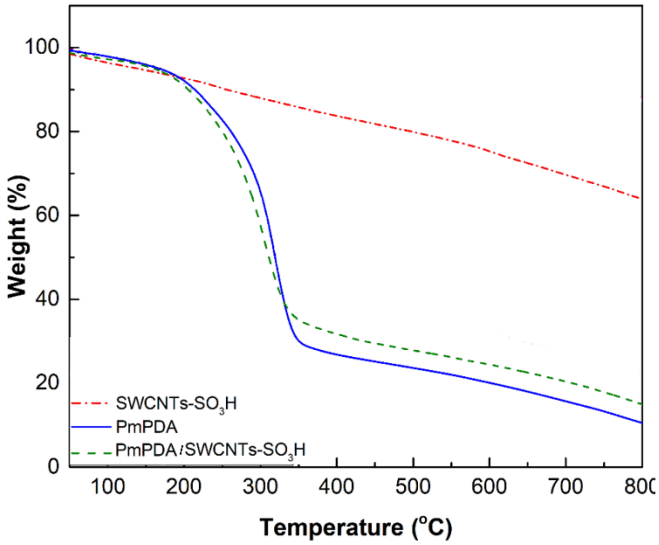

Figure 7. TGA cureves of PmPDA, SWCNTs-SO_3H, and PmPDA/SWCNTs-SO_3H nanocomposite.

3.2. Nonlinear optical properties

The rapid development of nanoscience and nanotechnology has provided several new opportunities for nonlinear optics [24]. A growing number of nanomaterials have been shown to possess remarkable nonlinear optical properties (NOPs); this promotes the design and fabrication of nano and nano-scale optoelectronic and photonic devices [25]. Nonlinear optics is widely used in many fields such as in laser technology, light aspects of communication, information and image processing and storage, and optical computing [26]. Since nonlinear optics has been widely used in these areas, nonlinear optics has great value and far-reaching scientific significance [27]. To do this, there are several methods for experimentally determining nonlinear optical parameters [28,29]. Nonlinear refraction and nonlinear absorption of the materials are the phenomena of major interest [30]. The Z-scan technique can be considered the gold standard for measuring nonlinear refraction and nonlinear absorption coefficients [31,32] and it has been used to study the nonlinear properties of a wide range of optical materials. In this paper, to prevent sedimentation of the nanoparticles, nanofluids of each sample were prepared. A two-step method was used to prepare the nanofluids from each sample. To prepare a nanofluid with a concentration of 0.3 mg/mL, the first 0.3 mg of each sample was added to 1 mL of dimethylsulfoxide (DMSO) solvent. The mixtures were then subjected to magnetic stirring, initially without agitation, then at specified time intervals until stable nanofluids were obtained. Nanofluids with concentrations of 0.5 and 0.7 mg/mL were also prepared similarly.

To investigate the change in nonlinear refractive indices with beam intensity, this experiment was performed at four different initial intensities. Two intensity-reducing filters were utilized to generate the different intensities, which were measured using a PM 100 intensity meter. The four incident intensities were 6.2, 17, 57.44, and 164.5 mW. The sample solution was then poured into a 1 mm thick cell and placed in the test arrangement. After measuring and recording the intensities passing through the sample using detectors, normalized intensity plots were obtained as a function of sample position along the Z-axis for the PmPDA, SWCNTs-SO_3H, and PmPDA/SWCNTs-SO_3H samples. **Table 1** shows the nonlinear optical parameters of the PmPDA sample at different concentrations (0.5, 0.3, and 0.7 mg/L) and incident laser intensities. Each concentration was tested four times with varying incident intensities. The results demonstrate the effect of intensity on the nonlinear optical response, with the nonlinear refractive index and nonlinear absorption coefficient dependent on the intensity. The negative nonlinear refractive index indicates self-defocusing behavior and nonlinear pulse reshaping capacity. Additionally, the negative nonlinear absorption coefficient ($\beta > 0$) signifies saturated absorption. Similar trends were observed for the SWCNTs-SO_3H and PmPDA/SWCNTs-SO_3H samples shown in **Tables 2** and **3**. The increasing optical transmission with higher intensity enables potential incorporation into optical limiters and switches in lasers. Since the materials exhibit self-defocusing, they can provide beam divergence control, being useful in the design of optical components and industrial/medical

laser systems. Importantly, the concentration and intensity changes were found to modulate the nonlinear properties of all three samples. As shown in **Tables 1, 2**, and **3**, variations in both parameters altered the nonlinear response of the PmPDA/SWCNTs-SO_3H, SWCNTs-SO_3H, and PmPDA samples. This affords flexibility in tailoring their nonlinear performance for laser engineering applications.

Table 1. Nonlinear optical parameters of P*m*PDA

$(\beta \pm 0.1) \times 10^{-5}(m/w)$	$(n_2 \pm 0.1) \times 10^{-3}(m^2/w)$	I(w/m^2)×10^3	C(mg/L)
-0.2411	-0.2289	164.5	0.3
-0.2196	-0.1668	57.44	
-0.0646	-0.1600	17	
-0.1066	-0.1569	6.2	
-0.1009	-0.1171	164.5	0.5
-0.0881	-0.1139	57.44	
-0.1635	-0.1659	17	
-0.2244	-0.1881	6.2	
-0.2844	-0.0415	164.5	0.7
-0.2750	-0.2048	57.44	
-0.0412	-0.0527	17	
-0.2189	-0.2035	6.2	

Table 2.Nonlinear optical parameters of SWCNTs-SO_3H

$(\beta \pm 0.1) \times 10^{-5}(m/w)$	$(n_2 \pm 0.1) \times 10^{-3}(m^2/w)$	I(w/m^2)×10^3	C(mg/L)
-0.2962	-0.2536	164.5	0.3
-0.4225	-0.2099	57.44	
-0.2607	-0.2680	17	
-0.2606	-0.1967	6.2	
-0.2004	-0.1853	164.5	0.5
-0.1377	-0.1204	57.44	
-0.2028	-0.1481	17	
-0.1966	-0.1639	6.2	
-0.2890	-0.1735	164.5	0.7
-0.2735	-0.1949	57.44	
-0.2496	-0.1397	17	
-0.1829	-0.1414	6.2	

Table 3. Nonlinear optical parameters of P*m*PDA/ SWCNTs-SO_3H

$(\beta \pm 0.1) \times 10^{-5}(m/w)$	$(n_2 \pm 0.1) \times 10^{-3}(m^2/w)$	I(w/m^2)×10^3	C(mg/L)
-0.1687	-0.1101	164.5	0.3
-0.1620	-0.1171	57.44	
-0.0616	-0.0541	17	
-0.0417	-0.0543	6.2	
-0.1379	-0.0966	164.5	0.5
-0.1573	-0.1714	57.44	
-0.1858	-0.1988	17	
-0.2784	-0.2058	6.2	
-0.1705	-0.1260	164.5	0.7
-0.1992	-0.1458	57.44	
-0.1581	-0.1226	17	
-0.1760	-0.1378	6.2	

4. Conclusions

In summary, an optically nonlinear poly(m-phenylene diamine) nanocomposite with incorporated sulfonated single-walled carbon nanotubes has been successfully developed. Materials characterization validated the fabrication methodology and modification of polymer properties like thermal stability and optical absorption upon nanotube addition. Notably, the nanocomposite was found to exhibit useful self-defocusing nonlinear optical behavior which could be tuned through simple variation of concentration and laser intensity parameters, unlike the pristine polymer. This platform presents opportunities for further fundamental studies elucidating the optical nonlinearity mechanisms

arising from synergistic effects between the conductive polymer matrix and integrated carbon nanotubes. Furthermore, harnessing the capacity for controlled self-defocusing by optimizing the distortion tolerance over wider intensity ranges and response times will enhance real-world applicability. With tailored nonlinearity, this nanocomposite material can serve as an optical limiter or switch to protect optics in laser systems from damage. Overall, these results represent progress toward fully unlocking the potential of carbon-polymer nanocomposites for photonic technologies through detailed understanding and control over the optical properties.

Authors' contributions

S. Rahimi: Data analysis and experimental. Y. Rajabi: Supervisor, Write the original draft and edit it.

Declaration of competing interest

The authors declare no competing interest.

Funding

This paper received no funding.

Data availability

Data will be made available on request.

References

[1] P. Yu, R.Y. Bao, X.J. Shi, W. Yang, M.B. Yang, Self-assembled high-strength hydroxyapatite/graphene oxide/chitosan composite hydrogel for bone tissue engineering, Carbohydr. Polym. 155 (2017) 507–515.
[2] M. Peyvandtalab, E.N. Zare, M. Jabbari, G. Heidari, Carboxymethyl dextrin-grafted-poly(aniline-co-m-phenylenediamine)@Fe3O4/CuO bionanocomposite: Physico-chemical characteristics and antioxidant, antibacterial, and cytotoxicity studies for potential biomedicine, Eur. Polym. J. 186 (2023) 111862.
[3] A. Ghahremanloo, E.N. Zare, F. Salimi, P. Makvandi, Electroconductive and photoactive poly(phenylenediamine)s with antioxidant and antimicrobial activities for potential photothermal therapy, New J. Chem. 46 (2022) 6255–6266..
[4] A. Tiwari, Y. Sharma, S. Hattori, D. Terada, A.K. Sharma, A.P.F. Turner, H. Kobayashi, Influence of poly(n-isopropylacrylamide)-CNT-polyaniline three-dimensional electrospun microfabric scaffolds on cell growth and viability, Biopolymers. 99 (2013) 334–341.
[5] H. Jing, E. Sahle-Demessie, G.A. Sorial, Inhibition of biofilm growth on polymer-MWCNTs composites and metal surfaces, Sci. Total Environ. 633 (2018) 167–178.
[6] S.G. Dhole, S.A. Dake, T.A. Prajapati, S.N. Helambe, Effect of ZnO filler on structural and optical properties of polyaniline-ZnO nanocomposites, Procedia Manuf. 20 (2018) 127–134.
[7] M. Khairy, M.E. Gouda, Electrical and optical properties of nickel ferrite/polyaniline nanocomposite, J. Adv. Res. 6 (2015) 555–562.
[8] Y. Zhang, Y. Wang, S. Qi, S. Dunn, H. Dong, T. Button, Enhanced discharge energy density of rGO/PVDF nanocomposites: The role of the heterointerface, Appl. Phys. Lett. 112 (2018).
[9] A.N. Gheymasi, Y. Rajabi, E.N. Zare, Nonlinear optical properties of poly (aniline-co-pyrrole)@ ZnO-based nanofluid, Opt. Mater. (Amst). 102 (2020) 109835.
[10] S. Dadkhah, Y. Rajabi, E.N. Zare, Thermal lensing effect in laser nanofluids based on poly (aniline-co-ortho phenylenediamine)@TiO2 interaction, J. Electron. Mater. 50 (2021) 4896–4907.
[11] M. Liu, H.S. Quah, S. Wen, J. Wang, P.S. Kumar, G. Eda, J.J. Vittal, W. Ji, Nonlinear optical properties of a one-dimensional coordination polymer, J. Mater. Chem. C. 5 (2017) 2936–2941.
[12] O. Muller, C. Hege, M. Guerchoux, L. Merlat, Synthesis, characterization and nonlinear optical properties of polylactide and PMMA based azophloxine nanocomposites for optical limiting applications, Mater. Sci. Eng. B. 276 (2022) 115524.
[13] Y. Wei, X. Ling, L. Zou, D. Lai, H. Lu, Y. Xu, A facile approach toward preparation of sulfonated multi-walled carbon nanotubes and their dispersibility in various solvents, Colloids Surfaces A Physicochem. Eng. Asp. 482 (2015) 507–513.
[14] M. Safa, Y. Rajabi, M. Ardyanian, Influence of preparation method on the structural, linear, and nonlinear optical properties of TiN nanoparticles, J. Mater. Sci. Mater. Electron. 32 (2021) 19455–19477.
[15] M.T. Hosseinzadeh, A. Hosseinian, Novel thin film composite nanofiltration membrane using monoethanolamine (MEA) and diethanolamine (DEA) with m-phenylenediamine (MPD), J. Polym. Environ. 26 (2018) 1745–1753.
[16] H. Yu, Y. Jin, Z. Li, F. Peng, H. Wang, Synthesis and characterization of sulfonated single-walled carbon nanotubes and their performance as solid acid catalyst, J. Solid State Chem. 181 (2008) 432–438.
[17] L. Zhang, L. Chai, J. Liu, H. Wang, W. Yu, P. Sang, pH manipulation: a facile method for lowering oxidation state and keeping

good yield of poly (m-phenylenediamine) and its powerful Ag+ adsorption ability, Langmuir. 27 (2011) 13729–13738.
[18] N. Badawi, M. Bhatia, N. Agrawal, S. Bashir, S. Ramesh, K. Ramesh, M. Bhuyan, Highly conductive-sensitive, single-walled carbon nanotubes–poly (3, 4-ethylenedioxythiophene) polystyrene sulphonate-coated cotton thread for thermally stable fabric and wearable e-textiles, Bull. Mater. Sci. 46 (2023) 208.
[19] B. Duran, G. Bereket, M. Duran, Electrochemical synthesis and characterization of poly (m-phenylenediamine) films on copper for corrosion protection, Prog. Org. Coatings. 73 (2012) 162–168.
[20] S. Bilal, R. Holze, In situ UV–vis spectroelectrochemistry of poly (o-phenylenediamine-co-m-toluidine), Electrochim. Acta. 52 (2007) 5346–5356.
[21] Y.-W. Lin, T.-M. Wu, Synthesis and characterization of externally doped sulfonated polyaniline/multi-walled carbon nanotube composites, Compos. Sci. Technol. 69 (2009) 2559–2565.
[22] F.B. Kheyrabadi, E.N. Zare, Antimicrobial nanocomposite adsorbent based on poly(meta-phenylenediamine) for remediation of lead (II) from water medium, Sci. Rep. 12 (2022) 1–14.
[23] C.Y. Du, T.S. Zhao, Z.X. Liang, Sulfonation of carbon-nanotube supported platinum catalysts for polymer electrolyte fuel cells, J. Power Sources. 176 (2008) 9–15.
[24] A. Di Francescantonio, A. Zilli, D. Rocco, L. Coudrat, F. Conti, P. Biagioni, L. Duò, A. Lemaître, C. De Angelis, G. Leo, All-optical free-space routing of upconverted light by metasurfaces via nonlinear interferometry, Nat. Nanotechnol. (2023) 1–8.
[25] B. Sephton, A. Vallés, I. Nape, M.A. Cox, F. Steinlechner, T. Konrad, J.P. Torres, F.S. Roux, A. Forbes, Quantum transport of high-dimensional spatial information with a nonlinear detector, Nat. Commun. 14 (2023) 8243.
[26] K. Ji, Q. Zhong, L. Ge, G. Beaudoin, I. Sagnes, F. Raineri, R. El-Ganainy, A.M. Yacomotti, Tracking exceptional points above the lasing threshold, Nat. Commun. 14 (2023) 8304.
[27] M.H.M. Ara, H. Akheratdoost, E. Koushki, Self-diffraction and high nonlinear optical properties of carbon nanotubes under CW and pulsed laser illumination, J. Mol. Liq. 206 (2015) 4–9.
[28] M.H.M. Ara, S. Salmani, M. Esmaeilzadeh, S.H. Mousavi, E. Koushki, K. Shakouri, Optical characterization of Erioglaucine using z-scan technique, beam radius variations and diffraction pattern in far-field, Curr. Appl. Phys. 9 (2009) 885–889.
[29] M.D. Zidan, A.W. Allaf, A. Allahham, A. Al-Zier, Z-scan measurements of single walled carbon nanotube doped acetylenedicarboxylic acid polymer under CW laser, Opt. Laser Technol. 80 (2016) 72–76.
[30] D.N. Christodoulides, I.C. Khoo, G.J. Salamo, G.I. Stegeman, E.W. Van Stryland, Nonlinear refraction and absorption: mechanisms and magnitudes, Adv. Opt. Photonics. 2 (2010) 60–200.
[31] M. Sheik-Bahae, A.A. Said, E.W. Van Stryland, High-sensitivity, single-beam n 2 measurements, Opt. Lett. 14 (1989) 955–957.
[32]E. Koushki, M.H. Majles Ara, H. Akherat Doost, Z-scan technique for saturable absorption using diffraction method in γ-alumina nanoparticles, Appl. Phys. B. 115 (2014) 279–284.